- Technical Paper -

A BI-DIRECTIONAL CRACKING TEST OF HIGH PERFORMANCE FIBER REINFORCED CEMENTITIOUS COMPOSITE

Benny SURYANTO[*1], Kohei NAGAI[*2] and Koichi MAEKAWA[*3]

ABSTRACT

This paper describes an experimental program to assess the cracking characteristic of High Performance Fiber Reinforced Cementitious Composite (HPFRCC) after damage. Four-point bending tests were conducted on pre-damaged HPFRCC plates having different initial damage levels and orientations. The result showed three unique cracking characteristics: a bi-directional crack pattern, the discontinuity of the secondary cracks, and a relatively orthogonal cracking pattern. Moreover, the initial damage was found to have a significant influence on the macroscopic response of the plate.

Keywords: HPFRCC, bi-directional crack pattern, pre-damaged

1. INTRODUCTION

HPFRCC is classified as a class of cementitious materials that exhibits pseudo-strain hardening behavior in tension. A distintictive example is Engineered Cementitious Composite (ECC) which has been introduced since the last decade [1]. Past research has shown much improvement of mechanical tensile property, cracking characteristic, and failure mechanism of HPFRCC under static, cyclic, and fatigue loading condition [2]. Multiple cracks gradually form until the localization has started. As a result, the integrated composite behavior in tension is much elevated. The reason behind this phenomenon is that the matrix, fiber, and its bond were properly designed so that excellent fiber bridging mechanism in cracks is achieved. Therefore, any tensile stresses perpendicular to the crack planes could be satisfactorily transferred.

However, to date, little attention was paid to investigate HPFRCC behavior after damage. Indeed, degradation in performance is likely to happen when principal stress direction differs from the orientation of the existing damage. In this situation, tensile stress will not be the only stress transfer along cracks, but also the combined of shear and tensile stresses. Accordingly, both local shear slip and local shear transfer mechanism are present in addition to the well-recognized fiber bridging stress and crack opening displacement (COD) [3]. As a result, two possible mechanisms may occur. First, initial cracks govern the macroscopic behavior until failure, no other cracks occur in any other directions (hereafter referred to as secondary cracks). The other is that at the beginning, initial cracks actively govern the macroscopic behavior. Afterwards, the secondary cracks form in which either cracks may still active. Under these abovementioned circumstances, HPFRCC is still expected to show its superior ductile behavior.

As the practical use of HPFRCC has remarkably grown in recent years, it is important to recognize the generalized HPFRCC behavior in complex condition, for instance, HPFRCC behavior after damaged. In addition, further use of HPFRCC in complex loading conditions will require a generalized and reliable numerical analysis framework. The well-established analysis framework of reinforced concrete (RC) has shown that a problematic nonlinearity behavior of RC could be much simplified by an exclusive treatment of multi-directional active crack concept in which the cracking criteria was one of the fundamental cores of the framework [4]. Therefore, the authors believe that it is important to first recognize the cracking characteristic of HPFRCC.

This study aims to investigate the bi-directional cracking characteristic of HPFRCC. Taking the advantage from its ductility in bending, a new yet simple technique is proposed by loading

*1 Ph.D. Student, Dept. of Civil Engineering, The University of Tokyo, M. E., JCI Member
*2 Assistant Prof., Dept. of Civil Engineering, The University of Tokyo, Dr. E., JCI Member
*3 Professor, Dept. of Civil Engineering, The University of Tokyo, Dr. E., JCI Member

pre-damaged plates under four-point bending test. Different initial damage conditions were introduced prior to the test. This experimental scheme is undertaken to emphasize the possible occurrence of arbitrary crack direction during the lifetime of structures. Furthermore, this macroscopic assessment also serves as fundamental step to further explore the mechanics of average stress transfer in cracks.

2. TEST PROGRAMS

2.1 Materials and Specimen Configuration

The HPFRCC tested in this study was ECC; basically made of cement, fly ash, chemical admixtures, and Polyvinyl Alcohol (PVA) fibers. The commercially available pre-mix type was used [5]. Eight plates in total were fabricated. The dimension and experimental parameters of each specimen are shown in Table 1. The first two specimens, namely standard specimens (S1 and S2), had a dimension of 250×400×20 mm. The rest (S3 to S8), namely main specimens, had a dimension of 410×550×20 mm. After casting, the specimens were fully covered with plastic sheet. After two days, all specimens were cured at temperature of 20°C and relative humidity of 60%, up to the test date (28 days from casting).

Table 1 Specimen Dimension and Main Parameters of Testing

ID	Dimension W mm	Dimension L mm	Dimension H mm	Initial Damage Orientation* Degree	Initial Damage Level % ε_{tu}	Specimen Type
S1	250	400	20	-	-	Standard
S2	250	400	20	-	-	Standard
S3	410	550	20	20	40	Main
S4	410	550	20	20	70	Main
S5	410	550	20	45	40	Main
S6	410	550	20	45	70	Main
S7	410	550	20	70	40	Main
S8	410	550	20	70	70	Main

* Measured from the plane normal to the long. direction of specimen after cut

As given in Table 1, the initial damage was of flexural cracking with two main parameters that were the levels and the orientations of the damage. Two initial damage levels were considered: Low Initial Damage (LID) and High Initial Damage (HID) levels, corresponding to 40% and 70% of ultimate tensile strain of standard specimens, respectively. To facilitate the damage orientation, each plate was cut aligning the damage approximately at 20°, 45°, and 70° from the plane normal to the longitudinal direction of the plate after cut. For a better illustration, Figure 1 provides the geometry, loading span, and layout of all plates. Specifically, the layout of the main plate shown in Fig. 1 corresponds to the plate shape before and after the cutting, as well as, the location of the supporting and the loading points of the applied four-point bending tests. The shaded area represents the shape of main specimen after cut, that is, similar to the standard one. For detailed explanations about the loading process, one should refer to the testing procedure given in the following subsection.

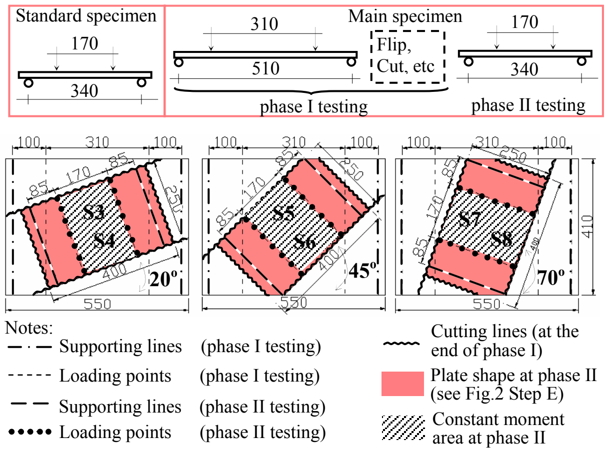

Fig.1 Geometry and Layout of All Plates

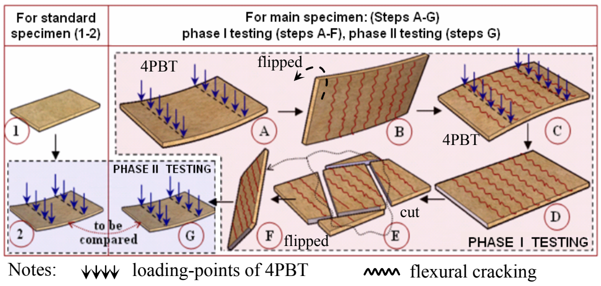

Fig.2 Testing Procedure for each Plate Type

2.2 Testing Procedure

A displacement-controlled four-point bending test was applied using a 200-kN universal testing machine at a constant rate of 0.5 mm per minute. As illustrated in Figure 2, two types of testing procedure were employed that was classified based on the specimen type. The complete description of the testing procedure is given as follows:

* For standard specimen (Steps 1-2, Fig. 2)

Four-point bending test was employed up to the failure (Step 2). The tests were conducted on a simply-supported condition with a span of 340 mm. Two-line loads as shown by groups of arrows were given at one-fourth of the span.

* For main specimen (Steps A-G, Fig. 2)

The testing consisted of two main loading phases. The first phase loading (Steps A-F) corresponded to the damage initialization in which four-point bending tests were initially performed on a simply supported condition with a span of 510 mm (see Steps A-D). The reversed loading (see Steps C-D) was employed to ensure the specimens remained flat. In this case, multiple cracks formed at soffit of each specimen. Later, the specimens were cut to become similar in size with the standard specimen (Step E) and flipped (Step F). From this condition, the second phase loading (Step G), which was a simply four-point bending test, was applied up to the failure of the specimen.

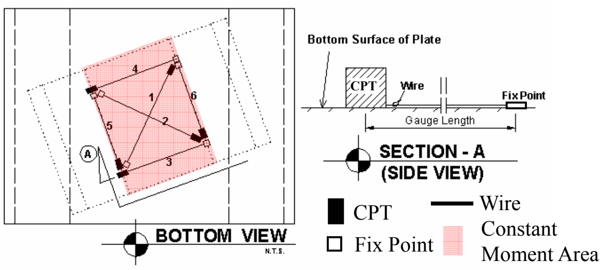

Fig.3 Instrumentation at Specimen S3

2.3 Data Measurement System

Two Linear Variable Differential Transducers (LVDTs) were used to measure the mid-span deflection. For strain measurement within the inner loading span, miniature cable position transducer (CPT, 19×19×10 mm – 15gr), was selected. Six CPTs were attached on the bottom surface of the specimen as illustrated in Figure 3.

2.4 Crack Pattern Analysis

The cracking patterns were qualitatively observed using fluorescent technique. The bottom surface of each specimen was treated with fluorescent dye after the test. Then, the specimens were placed under fluorescent black light tubes. No direct observation was made during the loading test.

3. TESTING RESULT

3.1 Determination of Initial Damage Level

The initial damage of main specimens (S3 to S8) was estimated from the bending test result of standard specimens (S1 and S2). The average tensile strain of the standard specimens at peak load was 1.23%. Thus, about 0.50% and 0.87% tensile strains were selected as the low and high initial damage levels of the main specimens (S3 to S8), respectively. Relatively stable saturation of peak load could be noticed in both specimens, from 1.23% to 1.62% tensile strains in average. Then, crack localization appeared and the load capacity abruptly dropped shortly afterward.

Table 2 Tensile Strain of Specimens

ID	Achieved Pre-Crack + Value %	Achieved Pre-Crack + Orientation* Degree	Strain at the Principal Loading Direction& At P_{max} %	Strain at the Principal Loading Direction& Before P Drop %
S1	-	-	1.21	1.44
S2	-	-	1.24	1.78
S3	0.55	24	1.42	1.51
S4	0.86	21	1.63	1.66
S5	0.47	44	1.27	1.38
S6	0.88	35	1.56	1.72
S7	0.50	63	0.86	0.92
S8	0.87	68	1.37	1.50

* pre-peak average values of principal strain direction
\+ correspond to Step A in Fig.2 & correspond to Step G in Fig.2

3.2 Load Displacement Relationship

The load-displacement behavior of each specimen is shown in Figure 4. The dash lines represent the result of standard specimens (S1 and S2) with no initial damage, while the other lines showed that of main specimens (S3 to S8) with various levels and orientations of initial damage.

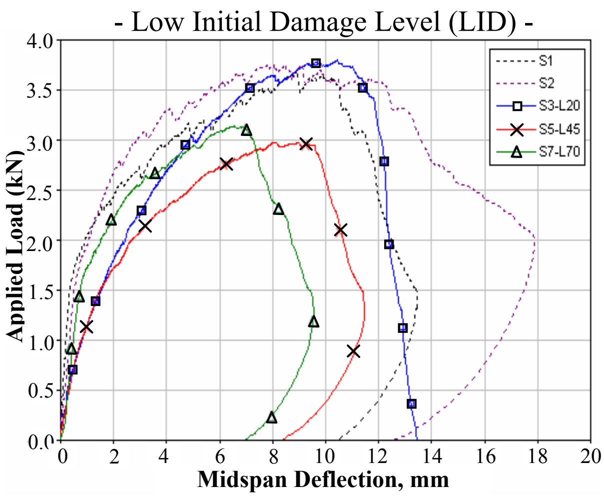

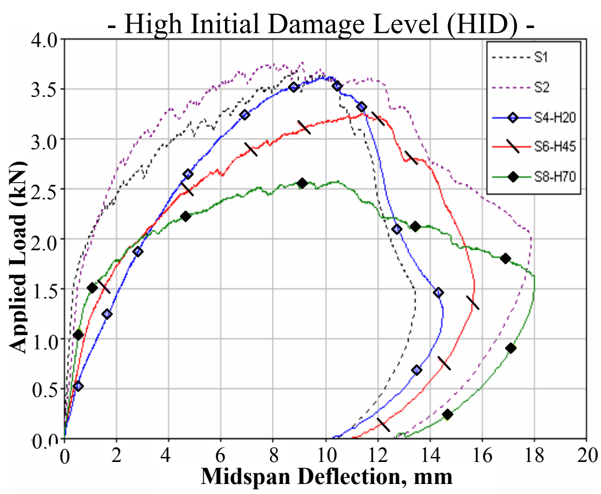

Fig.4 Comparison of Load-Deflection Curve of Tested Specimens: Low Initial Damage (top), High Initial Damage (bottom)

The result showed a considerable influence of initial damage on HPFRCC behavior after damage. In general, the initial damage orientation had affected more adversely the HPFRCC response than the initial damage level.

The initial damage orientation significantly reduced the strength capacity of HPFRCC. From Fig. 4, it was observed that specimen S5 to S8 (45^{o} and 70^{o} cases) experienced the most significant reduction of strength under similar initial damage level, which the largest reduction was around 30%. Both specimen S7 and S8 showed a clear flexural cracking (turning point). On the other hand, S3 and S4 (20^{o} case) showed relatively similar strength capacity compared to the standard specimens. Furthermore, the initial damage orientation also significantly affected the initial stiffness. The lower the orientation, the more stiffness degradation occurs, for example S3 and S4 showed the most significant reduction (around 65% reduction) under similar initial damage level.

The initial damage level, however, showed some influences on both mid-span deflection and tensile strain at the peak load in which the values of all main specimens with high initial damage level (S4, S6, and S8) were always higher than that of the standard specimens.

3.2 Uni-Directional Cracking Characteristic

The uni-directional crack pattern of all specimens (S1 to S8), after the first four-bending test, represents the cracking characteristic of HPFRCC with no initial damage.

For the standard specimen (S1 and S2), the crack development of specimen S1 was different than that of specimen S2. Specimen S1 had relatively uniform cracks. Crack localization initiated from the preceding cracks was close to each others. As a result, the final localized crack appeared almost parallel to the other cracks. On the other hand, specimen S2 had less uniform cracks than specimen S1. The final localized crack in specimen S2 was inclined, approximately 20^{o} relative to the other cracks. Several secondary fine cracks were found in the vicinity of localized cracks.

For the main specimen (S3 to S8), Figure 5 gives the sketch of the initial damage. The crack spacing was obtained from the observation after the test whereas the crack orientation was determined from the pre-peak average values of principal strain direction during the phase I testing (see Table 2). Ideally, the principal strain direction of a specimen, which is orthogonal to crack orientation, is equal to the principal stress direction applied to the specimen. In this study, the variation was one to ten degrees different (see Fig. 5) from the pre-defined value given in Table 1. For comparison, the crack pattern observed after the test is depicted in Figure 6. In most cases, the initial crack pattern is uniform. Nevertheless, specimen S6 had the least uniformity in which several crack branches were found. The calculated crack orientation was well consistent with the observed crack pattern appearance, representing the average of actual crack distribution quantitatively.

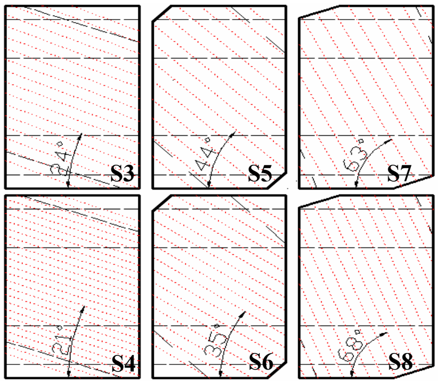

Note:
* For specimen shape, refer to Fig. 1.
* S3, S5, S7 represent Low Initial Damage (LID) level.
* S4, S6, S8 represent High Initial Damage (HID) level.

Fig.5 Damage pattern after Pre-Crack Stage

3.3 Bi-Directional Cracking Characteristic

The bi-directional cracking characteristic presented herein represents the cracking characteristic of main specimens (S3 to S8), which had different pre-damaged conditions (illustrated in Fig. 5), and then was subjected to further loading. For all specimens, three distinctive cracking behaviors were observed as shown in Fig. 6. First, bi-directional multiple crack patterns were observed, primary cracks and then secondary ones, with different orientations. Second, the initial cracks were uniform and continuous, while the secondary cracks were visibly discontinuous. Third, the orientation of secondary cracks appeared to be always somewhat orthogonal to the direction of first cracks regardless the orientation of the new principal stress direction, with the variation of 5^{o} to 15^{o}. This variation appears similar in each case of initial damage orientation.

The new principal stress direction had a significant influence to the crack localization appearances. Both S3 and S4 (20^{o} case) showed localization of cracks most likely at the initial cracks. On the other hand, it appeared at most of secondary cracks in both S7 and S8 (70^{o} case). Nevertheless, both S5 and S6 (45^{o} case) showed a mixed appearance. As the initial crack of specimen S6 formed some branches, the initial cracks oriented at a slight angle tended to have a larger opening than the other ones.

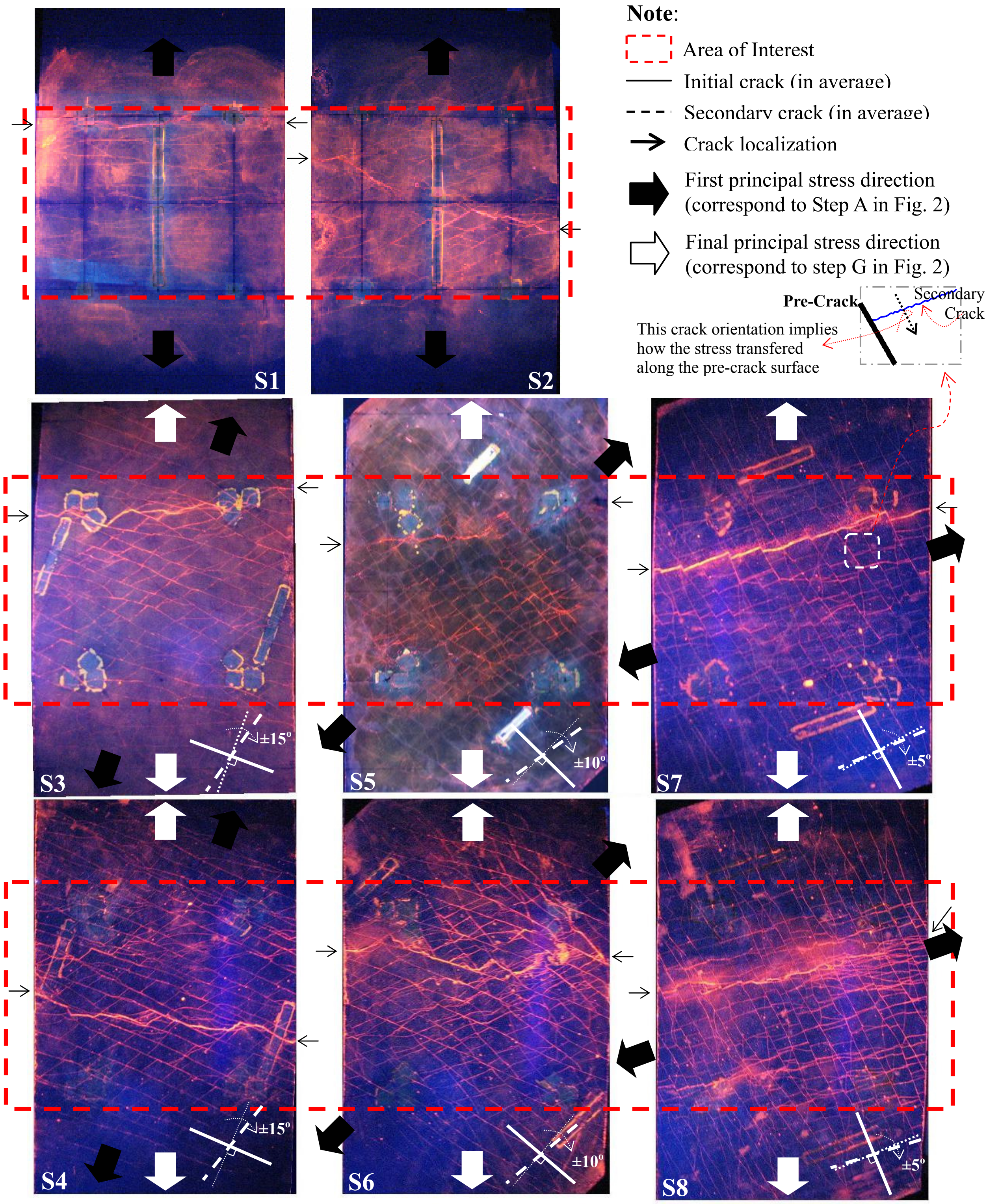

Fig.6 Crack Pattern by the End of the Testing (showing the bottom surface of the specimens)

4. DISCUSSION

The result shows that HPFRCC performance, represented by ECC herein, is greatly influenced by initial damage conditions (the term "performance" here refers to the strength and its corresponding mid-span deflection and tensile strain at the principal direction). Figure 7 gives the relationship between the performance ratio of the tested pre-damaged specimens' results normalized by the corresponding values of no damage specimens and the calculated initial damage orientation determined from the average of pre-peak principal strain direction. Apparent strength degradation was observed in both 45° and 70° initial damage orientation cases, in which the strength ratio was in a range of 0.70 to 0.85. This means that presence of shear stress in a crack plane will be dominant only when the proportion of the applied shear stress is similar or higher than the applied normal stress value. In most cases, however, a large value of mid-span deflection and its corresponding tensile strain in the principal stress direction still could be observed, which most of the ratio are similar or greater than 1.0 (only 1 case has 0.75 ratio). This phenomenon may correspond to the well distribution of cracks, showing that HPFRCC is still relatively ductile after damage.

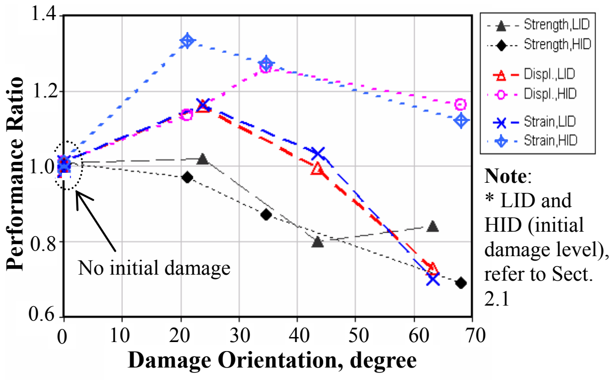

Fig.7 Performance Ratio under Various Initial Damage Levels and Orientations

In general, the crack pattern appeared in a zigzag shape relatively orthogonal to the new principal stress direction. Other than the initial and the secondary cracks, no other cracks were formed normal to the new principal stress direction, which is, in contract with the cracking characteristic of reinforced concrete member subjected to multi-directional of loading. In fact, the secondary cracks formed closer to the smallest section of matrix between two initial cracks. This secondary crack orientation reflects how the stress developed in the matrix between two initial cracks that mainly come from the stresses transferred by the embedded fibers as well as the negligibly friction between the crack planes.

5. CONCLUSIONS

A new yet simple experimental program has been proposed to obtain the cracking characteristic of HPFRCC after damage condition, an approach to evaluate its behavior in a complex loading condition. The following conclusion can be drawn:

(1) Three unique cracking characteristics were found: bi-directional multiple crack patterns, a uniform and continuous initial crack pattern yet a distinctly discontinuous secondary crack pattern, and a relatively orthogonal cracking appearance.

(2) The initial damage orientation had a significant influence to the location of the final crack localization. Both specimens with 20° initial damage case showed propagation of crack localization at most of the initial cracks, whereas the specimens of 70° case showed the localization at most of the secondary cracks. Moreover, mixed appearances were found in specimens of 45°.

(3) The possible degradation in HPFRCC performance was pointed out, in which the initial damage orientation was found to have more significant influence on the HPFRCC performance than the initial damage level. Apparent strength degradation was observed at both 45° and 70° initial damage orientation cases.

(4) After pre-damaged, HPFRCC still exhibits ductile behavior as shown by the performance ratio of mid-span deflection and ultimate tensile strain in the principal stress direction. The least ductile response was found in case of low initial damage level with 70° initial damage orientation.

ACKNOWLEDGEMENT

The first author acknowledges the financial support (MEXT scholarship) from the Ministry of Education, Culture, Sports, Science and Technology Japan. The authors are also thankful to Kajima Technical Research Institute for supplying the ECC material.

REFERENCES

[1] JCI-DFRCC Committee, "DFRCC Terminology and Application Concepts," JACT, Vol. 1, Nov., 2003, pp.335-340

[2] Li, V. C., "On Engineered Cementitious Composites (ECC)," JACT, Vol. 1, Nov., 2003, pp.215-230

[3] Li, V. C. and Leung, C. K. Y., "Steady State and Multiple Cracking of Short Random Fiber Composites," ASCE J. Eng. Mech., Vol. 118, Nov., 1992, pp.224-2264

[4] Maekawa, K., Pimanmas, A. and Okamura H., "Nonlinear Mechanics of Reinforced Concrete," Spon Press, 2003, pp.18-68

[5] JSCE, "Recommendations for Design and Construction of High Performance Fiber Reinforced Cement Composite with Multiple Fine Cracks (HPFRCC)," Concrete Library 127, 2007, pp.129-135 (in Japanesse)